IJPRSE
Progressive Research
International Journal of Progressive Research in Science and Engineering
Volume-1, Issue-3, June-2020
www.ijprse.com

Design and Analysis of an Electro-Magnetic Clutch

Abhishek Chowdhary, Anupam Kumar, Sanket Kumar Singh

Student, Department of Mechanical Engineering, Birla Institute of Technology, Mesra, Ranchi, India.

Corresponding Author: abhishekc540@gmail.com

Abstract: - This paper presents the designing and analysis of an Electromagnetic Clutch. Engagement and disengagement of clutch is operated electrically but the torque is transmitted mechanically. It overcomes the problem of higher response time of mechanical clutches. In this paper we have discussed, in detail, various steps we followed to design an electromagnetic clutch -calculations, CAD, and analysis of parts of electromagnetic clutch. Static analysis is done on designed parts to ensure the safe operation of clutch and also fatigue analysis is done for estimating life of components. This paper also demonstrates about Magneto-static Analysis to know about Electromagnet characteristics like Magnetic Flux density and Force density.

Key Words: — Electromagnetic Clutch, Fatigue analysis, Magneto-static analysis, Response Time.

I. Introduction

Electromagnetic clutches are one of the most recent types. It is electrically incorporated and dissolved, but the mechanical transmission is mechanically. It is for the same reason that they are also called electro-mechanical clutches. Engagement and dissolution do not occur by mechanical linkage, as in the case of conventional mechanical linkage, but by the principle of electromagnetic induction. This type of clutch operates smoothly and rapidly as soon as the mechanical linkage is removed. For that reason, they are best suited for remote services. However, the activation energy is dissolved in the engagement coil as heat energy and thus there is a risk of overgrowth. Thus, the maximum operating temperature of the clutch is limited by the insulation of the coil.

II. Literature Review

Kakinuma (2005): He presented a detailed outline of the various parts and their construction, which needed to be assembled into an electromagnetic clutch.

Martin Steinberg (2008): In his paper he gave us an estimate of the air gap between an electromagnet and an armature that allows the clutch disc to be compressed.

C. H. Piao, Z. Y. Huang, J. Wang, and C. D. Cho (2010): It was stated that through proper optimization of the armature's shape, the static torque of Electromagnetic clutch can be improved.

E. Humphrey (2016): He studied and found that the coefficient of kinetic friction for the clutch friction lining material that is in contact with rough surface of pressure plate decreases with increasing slip speed and rising contact temperature.

Francesco Bucchiet (2016): He found out that there is a loss of transmitted torque with increasing temperature.

Naila Mikhail-Boules (2017): In this paper he stated that the torque that is transmitted by the Electromagnetic clutch is dependent on the clutch geometry and coil current and is independent of the shaft speed.

III. Components

The major components of the Electromagnetic Clutch are:

1. Stator
2. Rotor
3. Armature
4. Friction Lining
5. Spring Plate
6. Flange
7. Coil

Apart from these parts, several other parts such as rivets, circlip, ball-bearings, etc. are also used for different functions of the Clutch.

IV. Material Selection

The next step was to select the materials. The challenge was to decide the material of Friction Lining and Armature. So, decision matrices were created for the same.

Table 1 is the decision matrix to select the material of Friction

Lining while Table.2. is the decision matrix to select the material of Armature:

Table.1. Decision Matrix for material of Friction Lining

Properties	**W.F.**	**Asbestos**	**Non-Asbestos**
Coefficient of Friction	1	0	1
Strength	1	1	1
Health hazardous	2	0	2
Temperature resistance	1	1	0
Total		2	4

Table.2. Decision Matrix for material of Armature

Properties	**W.F.**	**Mild Steel**	**Alloy Steel**
Hysteresis Loss	1	0	1
Cost	1	1	0
Availability	1	1	0
Total		2	1

Based on the decision matrices and considering several other factors the material for rotor, stator, armature and flange was selected to be Mild Steel while the material for friction lining was selected to be Non-Asbestos.

V. CALCULATIONS

The prime mover is being assumed to be a 10 HP Engine that produces a maximum torque of 20 N-m at 2600 RPM. Then,

Data known:

Torque to be transmitted (M_t) = 20 N-m

Power of Prime Mover (P) = 7460 W

Co-efficient of friction between Armature and Friction Lining (μ) = 0.2

Permissible intensity of pressure of Friction Lining (P_a) = 0.7 N/mm^2

Data Assumed:

Inner Diameter of Friction Lining (d_o) = 50 mm

1. Calculation of Outer Diameter of Friction Lining**:**

Let D_o be the Outer Diameter of the Friction Lining. We know,

$$M_t = \frac{\pi \mu P_a d_o (D_o^2 - d_o^2)}{8}$$

$$\therefore D_o = \sqrt{\frac{8M_t}{\pi \mu P_a d_o}}$$

Substituting the values, we get, $D_o \approx 100$ mm

2. Calculation of Normal Force required to transmit Torque***:***

Let P_n be the Normal Force required. We know,

$$M_t = \frac{\mu P_n (D_o + d_o)}{4}$$

$$\therefore P_n = \frac{4M_t}{\mu (D_o + d_o)}$$

Substituting the values, we get, P_n = 2666.67 N

3. Calculation of Number of turns for Electromagnet:

Data known:

Current (I) = 1.2 A

Area of Friction Lining (a) = 4.71×10^{-3} m^2

Permeability of free space (μ_o) = $4\pi \times 10^{-7}$ Wb/A-m

Air Gap (δ) = 0.2 mm

Let number of turns = N

We know,

$$P_n = \frac{\mu_o a (N \times I)^2}{2\delta^2}$$

$$\therefore N = \sqrt{\frac{2P_n \delta^2}{I^2 \mu_o a}}$$

Substituting the values, we get, N ≈ 1200 turns

VI. CAD

Based on the data collected after calculations, the CAD models of the parts were designed in Solidworks 2019.

They are shown below:

International Journal of Progressive Research in Science and Engineering
Volume-1, Issue-3, June-2020
www.ijprse.com

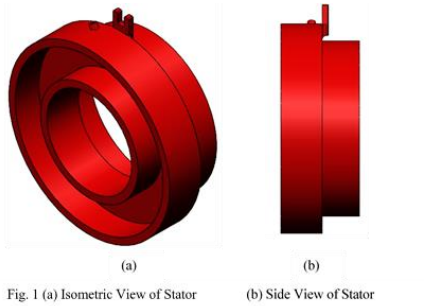

Fig.1. Shows the Isometric view and Side view of the Stator.

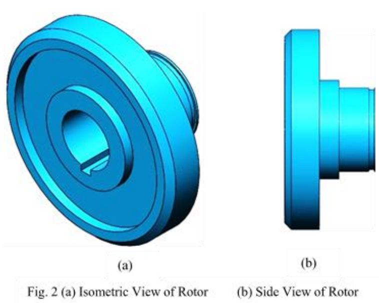

Fig.2. shows the Isometric view and Side view of the Rotor.

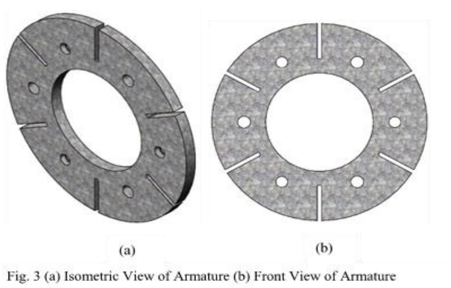

Fig.3. shows the Isometric view and Front view of the Armature.

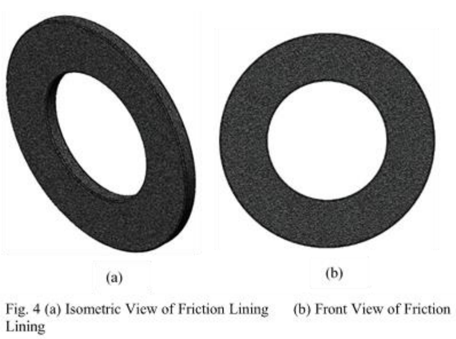

Fig.4. Shows the Isometric view and Front view of the Friction Lining.

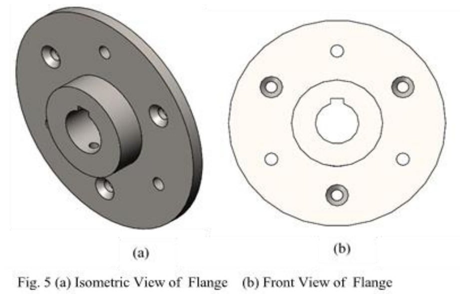

Fig.5. Shows the Isometric view and Side view of the Flange.

VII. FEA

Once the CAD was completed, the models were analyzed against the forces calculated earlier in HYPERMESH 14.0. The results are shown below:

A. Stator

Fig. 6 shows the stress in the total Stator and Fig. 7 shows the total displacement of the Stator.

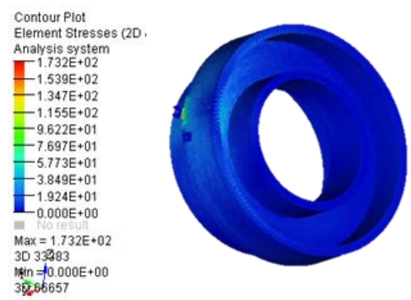

Fig.6. Total Stress in Stator

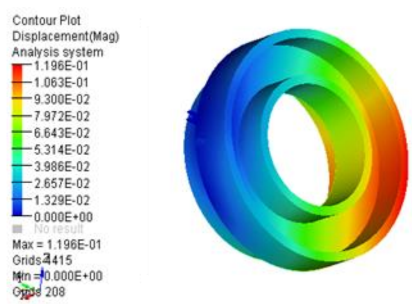

Fig.7. Total Displacement in Stator

As seen from Fig. 6, the maximum stress acting on Stator was found to be 34.5 MPa, and as seen from Fig.7, the maximum displacement is 0.01 mm.

B. Rotor

Fig. 8 shows the total stress in the Rotor and Fig. 9 shows the total displacement of the Rotor.

IJPRSE
Progressive Research
International Journal of Progressive Research in Science and Engineering
Volume-1, Issue-3, June-2020
www.ijprse.com

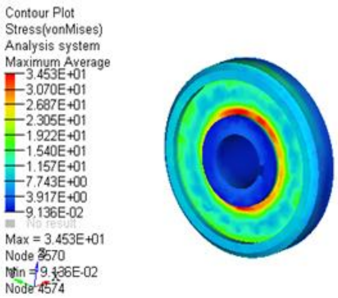

Fig.8. Total Stress in Rotor

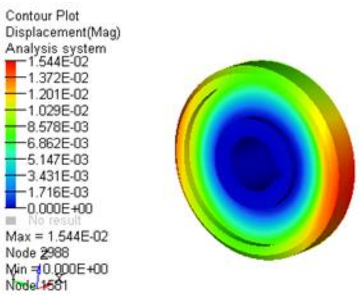

Fig.9. Total Deformation in Rotor

As seen from Fig. 8, the maximum stress acting on Rotor was found to be 173 MPa, and as seen from Fig.9, the maximum displacement is 0.12 mm.

C. Armature

Fig. 10 shows the total stress in the Rotor and Fig. 11 shows the total displacement of the Armature.

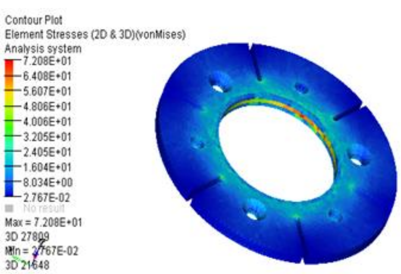

Fig.10. Total Stress in Armature

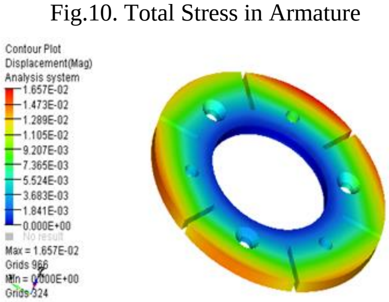

Fig.11. Total Deformation in Armature

As seen from Fig. 10, the maximum stress acting on Armature was found to be 72.08 MPa, and as seen from Fig.9, the maximum displacement is 0.016 mm.

D. Flange

Fig. 12 shows the total stress in the Flange and Fig. 13 shows the total displacement of the Flange.

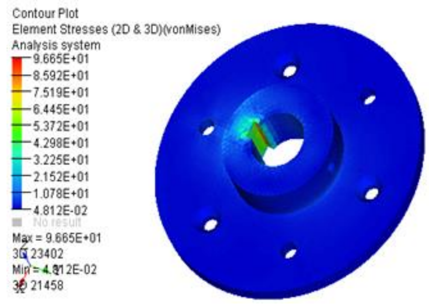

Fig.12. Total Stress in Flange

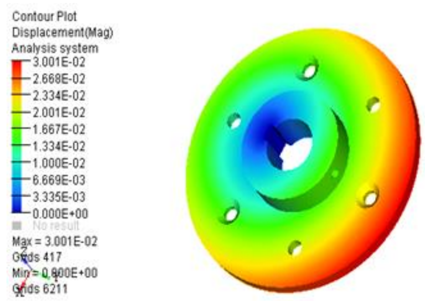

Fig.13. Total Deformation in Flange

As seen from Fig. 12, the maximum stress acting on Flange was found to be 96.65 MPa, and as seen from Fig.13, the maximum displacement is 0.03 mm.

E. Fatigue Analysis

Fig. 14 shows the Fatigue Analysis of the Stator and Fig. 15 shows the Fatigue Analysis of the Armature.

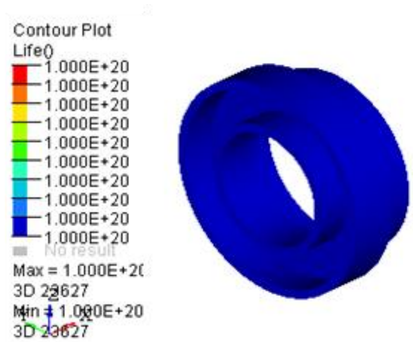

Fig.14. Fatigue Analysis of Stator

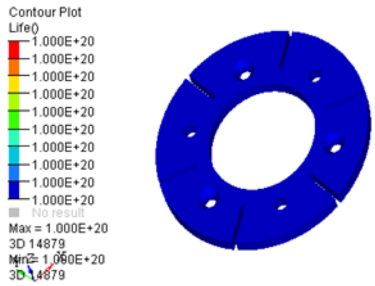

Fig.15. Fatigue Analysis of Armature

As seen from Fig. 14 and Fig. 15, both the Stator and the Armature has an Infinite Life.

VIII. ELECTROMAGNETIC CLUTCH ASSEMBLY

Once the analysis of the individual parts was complete, they were then assembled together in Solidworks 2019. This was done to identify any compatibility issues that may have arose later. All the fasteners used and key-slots designed were done keeping in mind the Industry Standards.

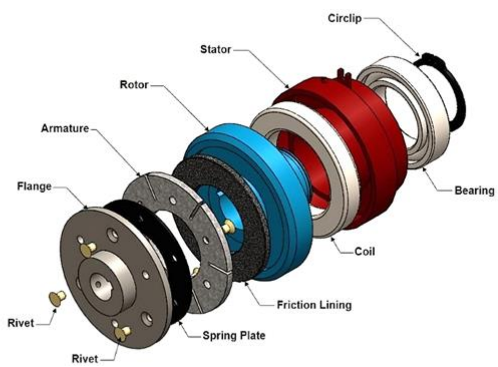

Fig. 16. Exploded View of the Clutch Assembly

IX. MAGNETO-STATIC ANALYSIS

A. Introduction

Magneto-statics is a subfield of the study of electromagnetism that deals with continuous magnetic fields.

In magneto-static analysis, Gauss's law for magnetism, that is, the deviation of the magnetic flux density is zero, and Ampere's law, that is, the curl of the magnetic field is equal to the constant electric current density, called the magnetic field and its calculation goes. Relative quantities due to electric current and permanent magnets. The Magneto-static analysis was performed on EMS 2020.

B. Procedure

The Magneto-static Analysis was performed on EMS 2020 by EMWorks. The steps followed to perform the analysis is shown in Fig. 17 below:

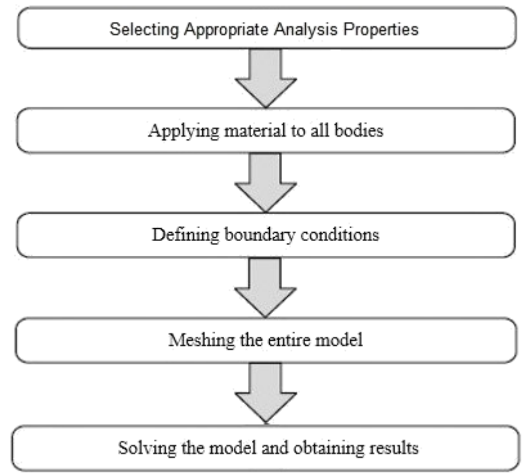

Fig. 17. Steps followed for the Magneto-static Analysis

Selecting Analysis Properties:

EMS 2020 provides a bunch of coupling analysis such as structural couplings, thermal couplings, etc. Selecting coupling allows the data to be computed but in turn it demands higher computation power and computing time.

Consequently, only relevant couplings had to be selected. As we only needed magneto-static results, there were no couplings we selected.

Applying Materials:

Appropriate materials were applied to all the parts of the Electromagnetic Clutch.

Nbr.	Part Name	Material Name	Permeability Type
1	AIR 1-1-Body 1 (Boss-Extrude1)	Air	Isotropic
2	AIR 2-1-Body 1 (Boss-Extrude1)	Air	Isotropic
3	Armature-1-Body 1 (CSK for M5 Flat Head Machine Screw1)	Mild Steel	Isotropic
4	Coil-1-Body 1 (Fillet1)	Copper	Isotropic
5	Flange-1-Body 1 (Cut-Extrude3)	Mild Steel	Isotropic
6	Friction Lining-1-Body 1 (Fillet1)	Non - Asbestos	Anisotropic
7	heavy duty external retaining ring_am-1-Body 1 (Body)	Mild Steel	Isotropic
8	radial ball bearing_68_skf-1-Body 1 (OuterRace)	AISI 4140	Isotropic
9	Rivet-2-Body 1 (Revolve2)	AISI 1010 Steel	Isotropic
10	Rivet-3-Body 1 (Revolve2)	AISI 1010 Steel	Isotropic
11	Rivet-4-Body 1 (Revolve2)	AISI 1010 Steel	Isotropic
12	Rivet-5-Body 1 (Revolve2)	AISI 1010 Steel	Isotropic
13	Rivet-6-Body 1 (Revolve2)	AISI 1010 Steel	Isotropic
14	Rivet-7-Body 1 (Revolve2)	AISI 1010 Steel	Isotropic
15	Rotor-1-Body 1 (Cut-Extrude2)	Mild Steel	Isotropic
16	Spring-1-Body 1 (Boss-Extrude1)	AISI 1018 Steel	Isotropic
17	Stator-1-Body 1 (Fillet3)	Mild Steel	Isotropic

Fig. 18. Material applied to the various parts

International Journal of Progressive Research in Science and Engineering
Volume-1, Issue-3, June-2020
www.ijprse.com

Boundary Conditions:

Boundary conditions are the most important aspect of any type of analysis. The following boundary conditions were defined for the analysis:

- Coil Properties: The properties of the wound coil were defined in this step. The wire was selected to be 22 AMG. Number of turns were taken to be 1200 and current to be 1.2 Amps.
- Direction of Current: In this step, the direction of Current-In and Current-Out of the coil was defined. The Current-In and Current-Out direction were taken to be same. Fig. 19 shows the direction of the Current with respect to the Rotor.

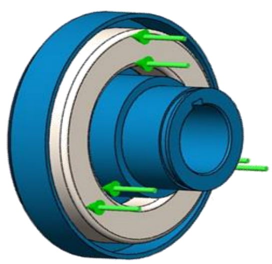

Fig. 19 Direction of Current-In and Current-Out

- Measurement of Force: In this step, the body on which the Lorentz Force was to be measured was defined. Armature was selected for this purpose. Fig. 20 shows the selection of the Armature.

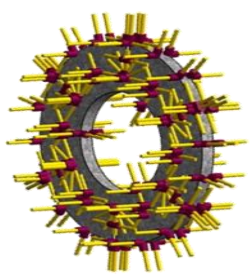

Fig. 20. Measurement of Lorentz Force

Meshing:

The most important part of meshing in EM solver is the meshing of the air gap. Air gaps are an integral part of electrical machines.

To facilitate the proper mesh of air gaps in EMS, we constructed a separate part or body for the air gaps. Then, we implemented a tight lattice control on the air gap portion, whose size was kept smaller than the surrounding air mesh size, where the lattice is usually thicker. This process is most recommended because it allows us to densely mesh around the interior air areas, where the area is important and roughly trap in the outer air areas where the area is usually small and decaying.

Following this step, we easily reduced the air gap and achieved a good accuracy without creating a large number of mesh elements, thus reducing the solver time. This ensured capture of field variation in the respective regions without creating a large number of elements. The mesh was manually adjusted using the EMS trap tool. Furthermore, we used the appropriate convergence criterion to obtain reasonable variance of the lattice size in the entire model.

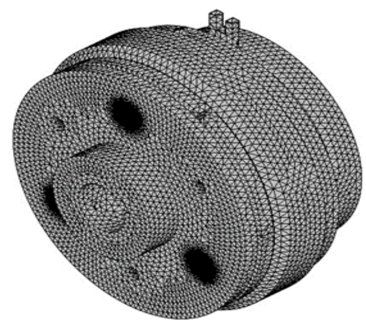

Fig. 21. Mesh View of the Assembly

Results:

Once all the parameters and the boundary conditions were set, the simulation was run and the following results were obtained:

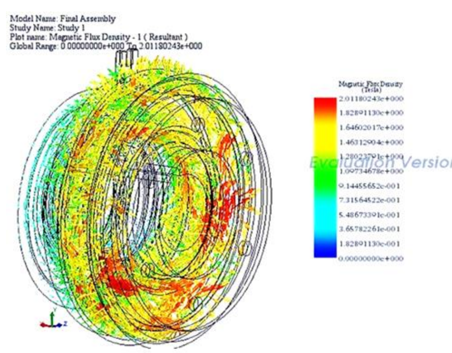

Fig. 22. Magnetic Flux Density

Fig. 22 shows the Magnetic Flux Density. We know that higher the flux density, stronger the magnet is at that area. From Uniform Wear Theory we know that greater pressure is required at the inner radius of the clutch plate.

From the figure above we can see that the flux density is maximum at the inner face thereby validating our design.

Fig. 23 shows the Force Density. To transmit a torque of 20 Nm, a clamping force of 2667 N is required.

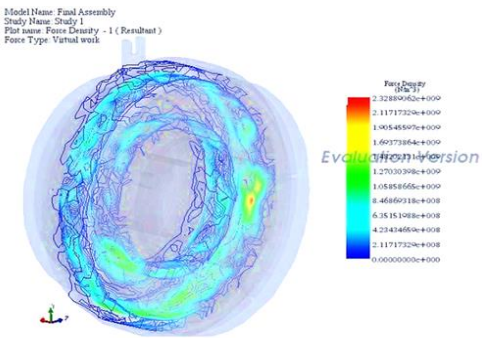

Fig. 23. Force Density

The average Force density when multiplied by the volume of Rotor gave a force of 2712 N. Thus, it is validated that the electromagnet is generating enough clamping force.

X. Conclusion

The various mechanical components of the electromagnetic clutch were successfully designed, analyzed and presented in this paper. All the aspects involved in the design of the electromagnetic clutch were carefully taken into consideration. Static analysis and fatigue analysis of the various components of the electromagnetic clutch was done to ensure safe design. Also, magneto-static analysis was performed to ensure desired magnetic force is generated as required for engagement of the clutch. Hence, by proper analysis we verified our design and calculations. Thus, without compromising on the safe design of clutch, an endeavor was made herein to present a simplified model of electromagnetic clutch.

References

[1]. O. P. C. Series and M. Science, “Design and control of electromagnetic clutch actuation system for automated manual transmission Design and control of electromagnetic clutch actuation system for automated manual transmission,” pp. 0–13, 2017.

[2]. A. Y. Krasil and A. A. Krasil, “Complementary products calculating the torque in an end magnetic clutch,” vol. 41, no. 7, pp. 26–28, 2005.

[3]. R. Karthik, S. Ashwin, and S. Raja, “Design and Working of Regenerative Clutch for Power Generation,” vol. 3, no. 11, pp. 1–4, 2017.

[4]. C. H. Piao, Z. Y. Huang, J. Wang, and C. D. Cho, “Torque Analysis and Shape Optimization of Electromagnetic Clutch C.H. Piao 1, 2,” pp. 122–126, 2010.

[5]. E. Diez-Jimenez, R. Rizzo, and E. Corral, “Review of Passive Electromagnetic Devices for Vibration,” vol. 2019, 2019.

[6]. E. Humphrey, “Clutch lining frictional characteristics under thermal tribodynamic conditions,” no. September 2016.

[7]. G. Wei and Z. Chengning, “Design of a High Torque Density Single-disc Electromagnetic Clutch,” 2010 Int. Conf. Electr. Mach. Syst., no. 1, pp. 1666–1669.

[8]. K. Saurabh and I. Ali, “Fabrication of Electromagnetic Clutches and Braking System,” 2017.

[9]. P. R. P. Kattimani, R. A. Shewate, R. M. Supe, C. Mukund, and P. S. Yewale, “Transmission Braking System by Using Electromagnetic Clutch,” pp. 24–29, 2018.

[10]. P. E. D. Herrmann, “United States Patent (19),” no. 19, 1991.

[11]. K. Nakano, “Tee RN,” vol. 1, no. 12, 2002.

[12]. C. F. Dynamics, “Magnetorheological AWD Clutches,” vol. 8.

[13]. D. Analysis, O. F. Electromagnetic, P. Clutch, N. M. General, M. Engineering, and M. Road, “No Title,” vol. 357, pp. 357–360, 1994.

[14]. U. States, “(12) Patent Application Publication ((43 10)) Pub.No.: US 2019,” vol. 1, 2019.

[15]. N. Fernando, “A Field Modulated Electromagnetic Clutch with Slip Control,” no. August 2017.

[16]. O. I. Abdullah and J. Schlattmann, “Thermal behavior of friction clutch disc based on uniform pressure and uniform wear assumptions,” vol. 4, no. 3, pp. 228–237, 2016.

[17]. Shapiro, Jessica. “The Basics of Electromagnetic Clutches and Brakes.” Machine Design, 9 Feb. 2016, www.machinedesign.com/archive/basics-electromagnetic-clutches-and-brakes.

[18]. Cserto, Tamas. “Electromagnetic Toothed Coupling Clutch.” The GrabCAD Community Library, Feb. 2017, grabcad.com/library/electromagnetic-toothed-coupling-clutch-1.

[19]. Alan, Warner. “Clutches and Brakes: Warner Electric Literature.” Clutches and Brakes | Warner Electric Literature, Apr.2009.

[20]. “Basic Requirements of Machine Elements.” Design of Machine Elements, by V. B. Bhandari, 4th ed., Tata McGraw-Hill, 2010, pp. 4–5.

[21]. “Friction Clutches.” Design of Machine Elements, by V. B. Bhandari, 4th ed., Tata McGraw-Hill, 2010, pp. 441–455.